The Function of Wnt Ligands on Osteocyte and Bone Remodeling

J.H. Du , S.X. Lin, X.L. Wu, S.M. Yang, L.Y. Cao, A. Zheng, J.N. Wu, and X.Q. Jiang

Appendix Materials and Methods.

Mouse Lines

Dmp1-Cre;*Wls*$^{flox/flox}$, referred to as "CKO" mice, were generated by crossing *Dmp1-Cre* mice (Lu et al. 2007) with *Wls*$^{flox/flox}$ mice (Zhu et al. 2012). *Wls*$^{flox/flox}$ mice were used for the control group with wild-type (*Wls*$^{flox/flox}$, referred to as "WT" mice) in the cohort studies. The floxed status of the *Wls* conditional allele was genotyped by PCR with the following primers: P1: 5'-ATACTTTTTCTGATCTGTTGT-3' and P2: 5'-AAGTTTTAATAGGTCTGTGTT-3'. The presence of *Dmp1-Cre* was identified by the primers F-5'-CCCGCAGAACCTGAAGATG-3' and R-5'-GACCCGGCAAAACAGGTAG-3'. All mice were housed in temperature-controlled specific pathogen free (SPF) conditions, with 12-h light/dark cycles, and were sacrificed at indicated time points. All animal protocols were approved by the Institutional Animal Care and Use Committee of the Ninth People's Hospital, Shanghai Jiao Tong University School of Medicine (No. HKDL2016319), which conforms with ARRIVE guidelines. Spontaneous bone fractures rendered the animals painful and immobile and necessitated their euthanasia as the humane endpoints following the guide of Institutional Animal Care and Use Committee of the Ninth People's Hospital, Shanghai Jiao Tong University School of Medicine.

Morphological and Biomechanical Analyses of Bones

At 3 wk, 8 wk and 3 mo of age, the bone mineral density (BMD) of femur, tibia and mandible of WT and CKO mice were evaluated using high-resolution radiography (Faxitron X-ray Corporation, Wheeling, IL). The whole skeletal CT images of WT and CKO mice at 6 mo were obtained using a Latheta LCT-200 X-ray CT scanner (Hitachi, Tokyo, Japan). Furthermore, three pairs of femoral trabecular and cortical bone, alveolar bone and mandible architecture of WT and CKO mice at 3 mo of age was assessed using a microcomputed tomography (micro-CT) system (Scanco Medical AG, Switzerland) according to the guidelines described. Three-point bending has been used for biomechanical testing of four pairs of normal and mutant femurs at 8 wk of age using a microcomputer control electronic universal testing machine (HY0230, Hengyi, Shanghai, China) (Jarvinen et al. 2005).

Histological and Serological Analyses

Briefly, sections were stained with hematoxylin-eosin (HE), terminal deoxynucleotidyl transferase dUTP nick end labeling (TUNEL, Roche), TRAP (Sigma-Aldrich) and other immunohistochemistry or immunofluorescence staining. The primary and secondary antibodies used in our study are listed in Appendix Table 1. For dynamic bone histomorphometric analysis,

double fluorescence labeling was performed as described previously (Wang et al. 2012). Briefly, calcein and alizarin red were administered to the 8-wk old mice by intraperitoneal injection at 7 d and 2 d before sacrifice, respectively. The mean distance between the two fluorescent labels was divided by the number of days (5) to calculate the mineral apposition rate (MAR), expressed as μm/d, n=3.

Enzyme-linked immunosorbent assay (ELISA) was used to determine serum biomarkers for C-terminal telopeptides of type I collagen (CTX-I, AC-06F1, IDS, Immunodiagnostic Systems plc, Tyne and Wear, UK), OPG (ELM-OPG, RayBiotech, Norcross, GA, USA), and RANKL (MTR00, R&D Systems, Minneapolis, MN, USA) of the WT and CKO mice at 8 wk or 6 mo of age following the manufacturer's instructions, n=4.

Osteogenic Induction and Coculture Assays

The osteocytic MLO-Y4 cell line were cultured and transduced with control-cherry-lentivirus (referred to as "Con-lenti") or *Wls*-cherry-lentivirus (referred to as "*Wls*-lenti"). Each group of MLO-Y4 osteocytic cell line was cultured in osteogenic medium consisting of ascorbic acid and β-glycerol phosphate. At day 7, calcium nodules were stained with Alizarin red (Sigma) and quantified by optical density (OD) values at 590 nm. Conditioned media from Con-lenti and *Wls*-lenti MLO-Y4 cells (referred to as "CCM" and "WCM") were collected at 24 h for further coculture experiments according to the previous method with slight modifications (Maycas et al. 2017). In detail, two groups of MLO-Y4 cells were exposed to serum-free α-MEM culture medium for 24 h. Then, the conditioned media was collected. Murine preosteoblastic MC3T3-E1 or murine RAW264.7 macrophages were cultured in CCM and WCM, with cells cultured in normal medium as a control group. The ALP activity and the osteogenic gene expression levels of MC3T3-E1 cells were assessed after 4 d of coculture. For osteoclast recruitment, a migration assay was performed using transwell chamber inserts (Corning Costar Corporation, Cambridge, MA). The osteoclastic differentiation of the cocultured RAW264.7 cells at 4 d was evaluated by the expression levels of osteoclastic differentiation-associated genes and TRAP staining after supplementation with 1,25-dihydroxyvitamin D3 (10^{-8} M; Sigma) (Zhao et al. 2002).

Quantitative Real-Time RT-PCR and Western Blotting Assay

The mRNA of bones or cells was extracted using the AxyPrep Multisource Total RNA Miniprep Kit (Axygen, Tewksbury, MA, USA) according to standard procedures. Specifically, for femur and tibia, the epiphysis, periosteum, and marrow were removed before the cortical bone mRNA was extracted and reverse-transcribed. Real-time PCR was performed on a Roche LightCycler 480 System (Roche, Basel, Switzerland). The samples were normalized to *Gapdh* expression. All primers are listed in Appendix Table 2. Western blot analysis was performed according to a standard protocol. Immunoreactive bands were visualized using an UVItec ALLIANCE4.7 gel imaging system.

Statistical Analyses

Repeated experiment results are presented as the means ± standard deviations. Comparisons

between 2 groups were made with a 2-tailed Student's t test, and differences among multiple groups were established by a 1-way analysis of variance (ANOVA) with Tukey's multiple comparisons test. $P < 0.05$ was considered statistically significant. All tests were performed with GraphPad Prism 6 software program (GraphPad Software Inc.).

Appendix Table 1. The primary, secondary antibodies and reagents used for antibody staining.

Reagent	Catalogue number	Dilutions/ Concentration
Anti-Wnt1 antibody	Abcam (Ab 15251)	1:100
Anti-Wnt7b antibody	Sigma-Aldrich (SAB2108321)	1:100
Anti-Wnt10B antibody produced in rabbit	Sigma-Aldrich (PRS4619)	1:100
Mouse/Rat Wnt-5a Antibody	R&D (AF645)	15 µg/mL
Wnt-5b Antibody (G-4)	Santa Cruz (Sc-376249)	1:50
GPR177(S-25)/Wntless antibody	Santa Cruz (Sc-133635)	1:50
Anti-Sp7 / Osterix antibody - ChIP Grade	Abcam (Ab 22552)	1:100
PY489-B-catenin	Developmental studies hybridoma bank (AB_10144551)	5µg/ml
Anti-Osteoprotegerin antibody	Abcam (Ab 9986)	0.5 µg/ml
Anti-RANKL antibody	Abcam (Ab 45039)	5 µg/ml
DAB	Sigma-Aldrich (D5637)	0.5mg/ml
VECTASTAIN® ABC-Peroxidase Kits	Vectorlabs (PK-4000)	-
Fluorescein (FITC) AffiniPure Goat Anti-Rabbit IgG (H+L)	Jackson ImmunoResearch (111-095-003)	1:100
Fluorescein (FITC) AffiniPure Goat Anti-Mouse IgG (H+L)	Jackson ImmunoResearch (115-095-003)	1:100
Cy™3 AffiniPure Goat Anti-Rabbit IgG (H+L)	Jackson ImmunoResearch (111-165-003)	1:100
Cy™3 AffiniPure Goat Anti-Mouse IgG (H+L)	Jackson ImmunoResearch (115-165-003)	1:100
Cy™3 AffiniPure Rabbit Anti-Goat IgG (H+L)	Jackson ImmunoResearch (305-165-003)	1:100

Appendix Table 2. The primer sequences used for quantitative real-time PCR.

Gene	Forward primer sequence (5' to 3')	Reverse primer sequence (5' to 3')
Gapdh	AAATGGTGAAGGTCGGTGTG	AGGTCAATGAAGGGGTCGTT
Wls	ACCGTGATGATATGTTTTCTG	TACCACACCATAATGATGAA
Col1a1	GCCTTGGAGGAAACTTTGCTT	GCACGGAAACTCCAGCTGAT
OC	TGCACCCAGATCCTATAGCC	CTCCATCGTCATCATCATCG
Opn	AGACTCCGGCGCTACCTT	CTCGTCACAAGCAGGGTTAAG
Dmp1	AGTGAGTCATCAGAAGAAAGTCAAGC	CTATACTGGCCTCTGTCGTAGCC
Rank	ATGAGCATCTCGGACGGT	CACACACTGTCGGAGGTAGG
Nfatc1	TCACCACAGGGCTCACTAT	GTTCATTCTCCAAGTAACCGT
Trap	CACCCTGAGATTTGTGGCTGT	CGGTTCTGGCGATCTCTTTG
Src	GTTGGGATAAGTGTCAGAGTG	GGGGTGATGTGTCAGTGAT
β-catenin	TCATGCGCTCCCCTCAGATG	AATCCACTGGTGACCCAAGC
Tcf1	ACATGAAGGAGATGAGAGCCA	CTTCTTCTTTCCGTAGTTATC
Axin2	GGTTCCGGCTATGTCTTTGC	CAGTGCGTCGCTGGATAACTC

Appendix Results.

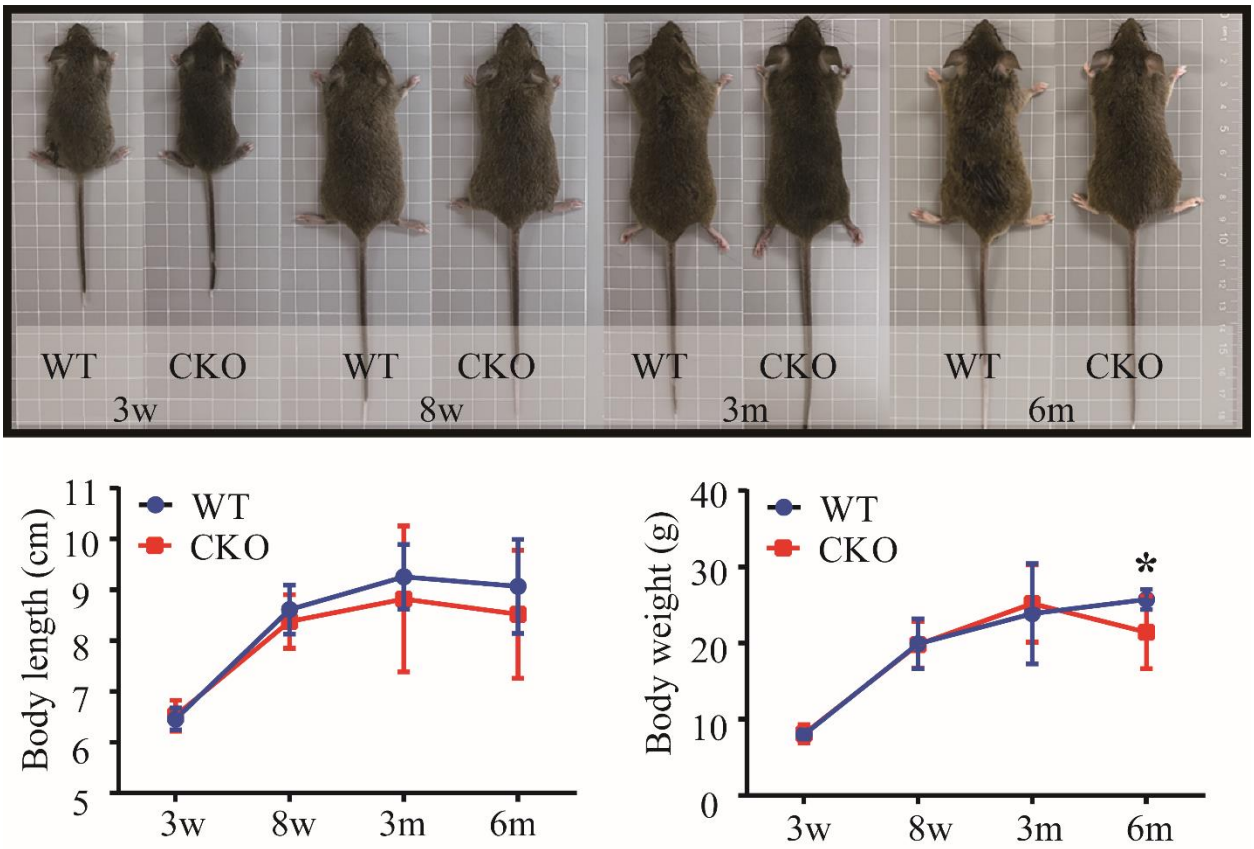

Appendix Figure 1. Body size, length and weight of WT and CKO at different ages. *P < 0.05, Student's t test, 3w n_{wt}=12, n_{cko}=10; 8w n_{wt}=20, n_{cko}=16; 3m n_{wt}=11, n_{cko}=5; 6m n_{wt}=12, n_{cko}=6.

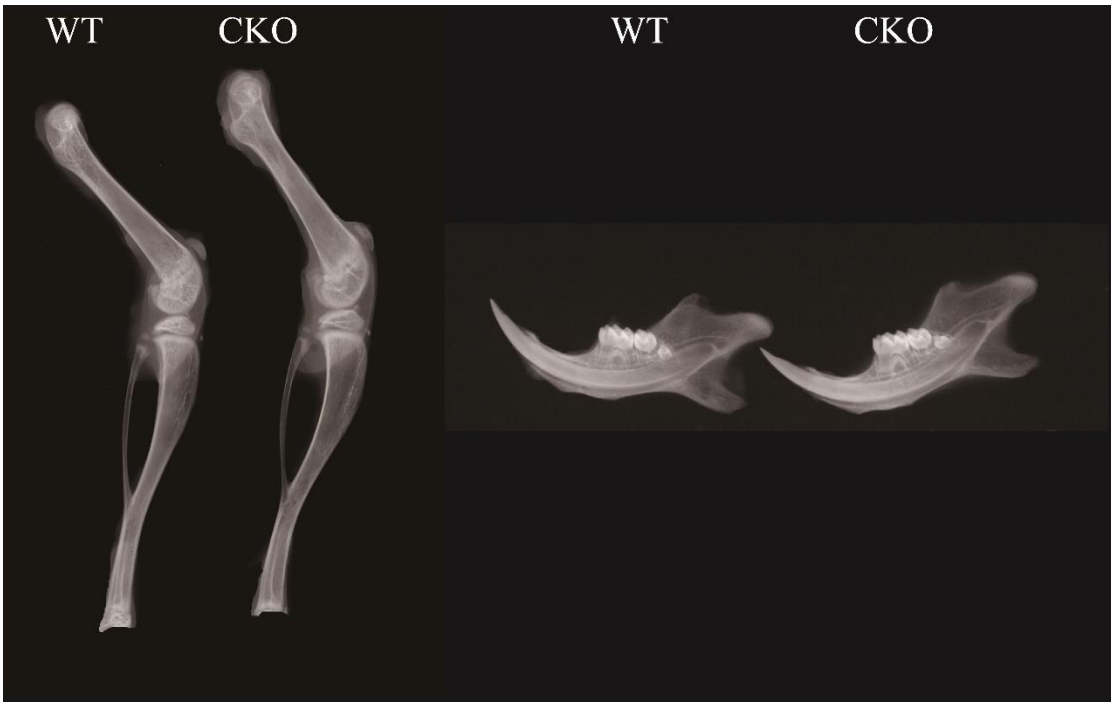

Appendix Figure 2. X-ray analysis for the bone mineral density (BMD) of the femur, tibia and mandible in WT and CKO mice at 3 wk of age.

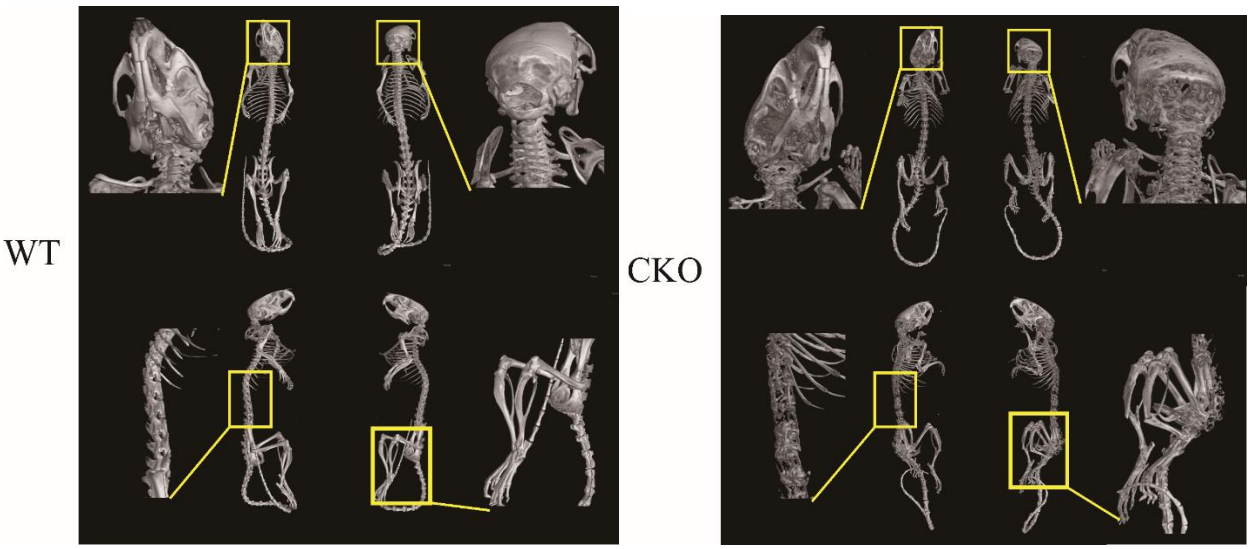

Appendix Figure 3. Whole skeleton micro-CT scanning analysis of the craniofacial bone, spine and long bone in WT and CKO mice at 6 mo of age.

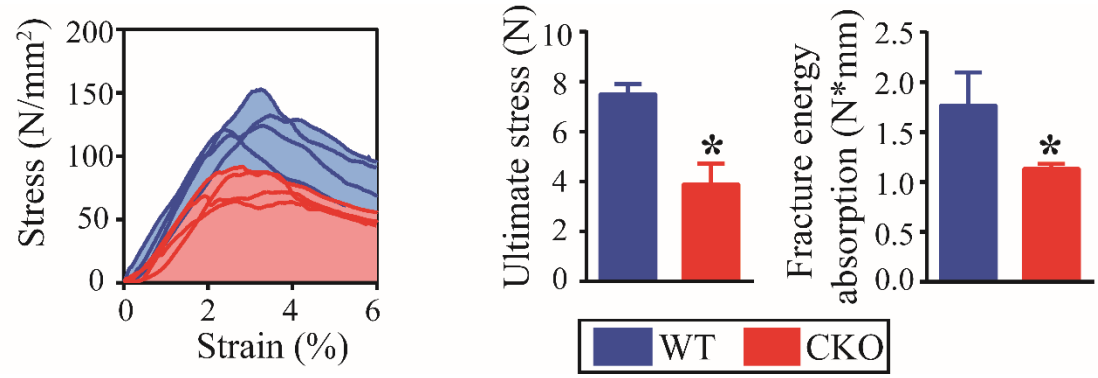

Appendix Figure 4. Three-point bending test of femur from WT and CKO mice at 8 wk of age. *P < 0.05, Student's t test, n=4.

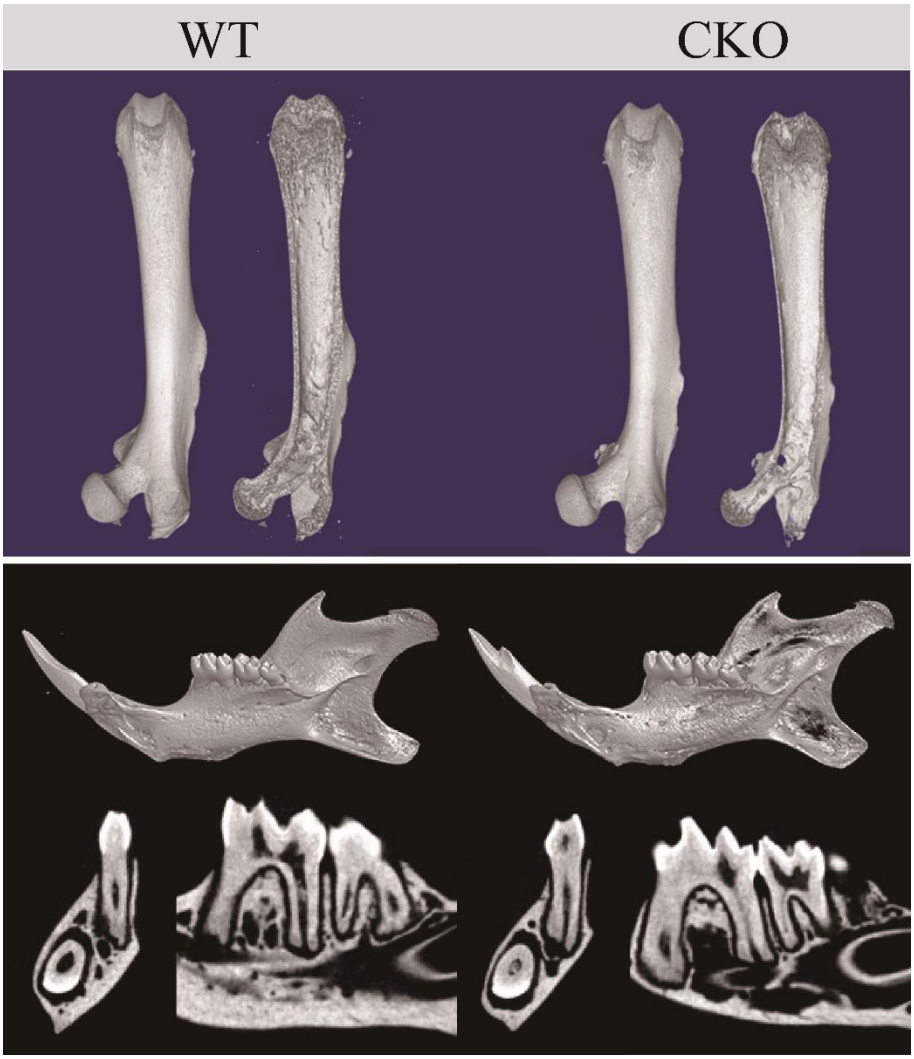

Appendix Figure 5. 3D and cross-section of micro-CT images of the femur and mandible from WT and CKO mice at 8 wk of age.

Appendix Table 3. Bone microstructure parameters of micro-CT in WT and CKO mice at 3 mo of age. Ct.Ar, Cortical cross-sectional bone area; Ct.Pm, cortical cross-sectional bone perimeter; Ct.Th, cortical bone thickness; BV/TV, the bone volume/total volume; BS/BV, bone surface/volume ratio; BS/TV, bone surface/total volume; Tb.Th, trabecular thickness; Tb.N, trabecular number, Tb.Sp, trabecular separation; BMD, bone mineral density. *P < 0.05, Student's t test, n=3.

	WT		CKO		
Cortical bone	Mean	SD	Mean	SD	Significant
Ct.Ar	0.93	0.05	0.63	0.02	*
Ct.Pm	12.33	1.08	13.18	0.66	-
Ct.Th	0.15	0.01	0.11	0.01	*
BMD	1.36	0.02	1.20	0.02	*
Trabecular bone	Mean	SD	Mean	SD	Significant
BV/TV	11.01	2.93	2.54	0.73	*
BS/BV	99.13	14.63	92.20	3.58	-
BS/TV	10.77	2.73	2.33	0.59	*
Tb.Th	0.04	0.01	0.04	0.00	-
Tb.N	2.80	0.75	0.58	0.17	*
Tb.Sp	0.18	0.03	0.56	0.05	*
BMD	0.21	0.04	0.09	0.01	*
Alveolar bone	Mean	SD	Mean	SD	Significant
BV/TV	77.24	1.77	56.55	4.93	*
BS/BV	15.10	0.38	22.52	2.18	*
BS/TV	11.66	0.35	12.66	0.12	*
Tb.Th	0.22	0.01	0.17	0.01	*
Tb.N	3.51	0.09	3.33	0.29	-
Tb.Sp	0.18	0.02	0.29	0.03	*
BMD	1.24	0.02	0.83	0.07	*
Mandibular bone	Mean	SD	Mean	SD	Significant
BV/TV	78.32	3.53	57.86	2.40	*
BS/BV	13.11	0.74	20.89	1.17	*
BS/TV	10.25	0.17	12.07	0.18	*
Tb.Th	0.29	0.01	0.18	0.01	*
Tb.N	2.73	0.02	3.20	0.08	*
Tb.Sp	0.15	0.01	0.17	0.01	-
BMD	1.33	0.07	0.90	0.04	*

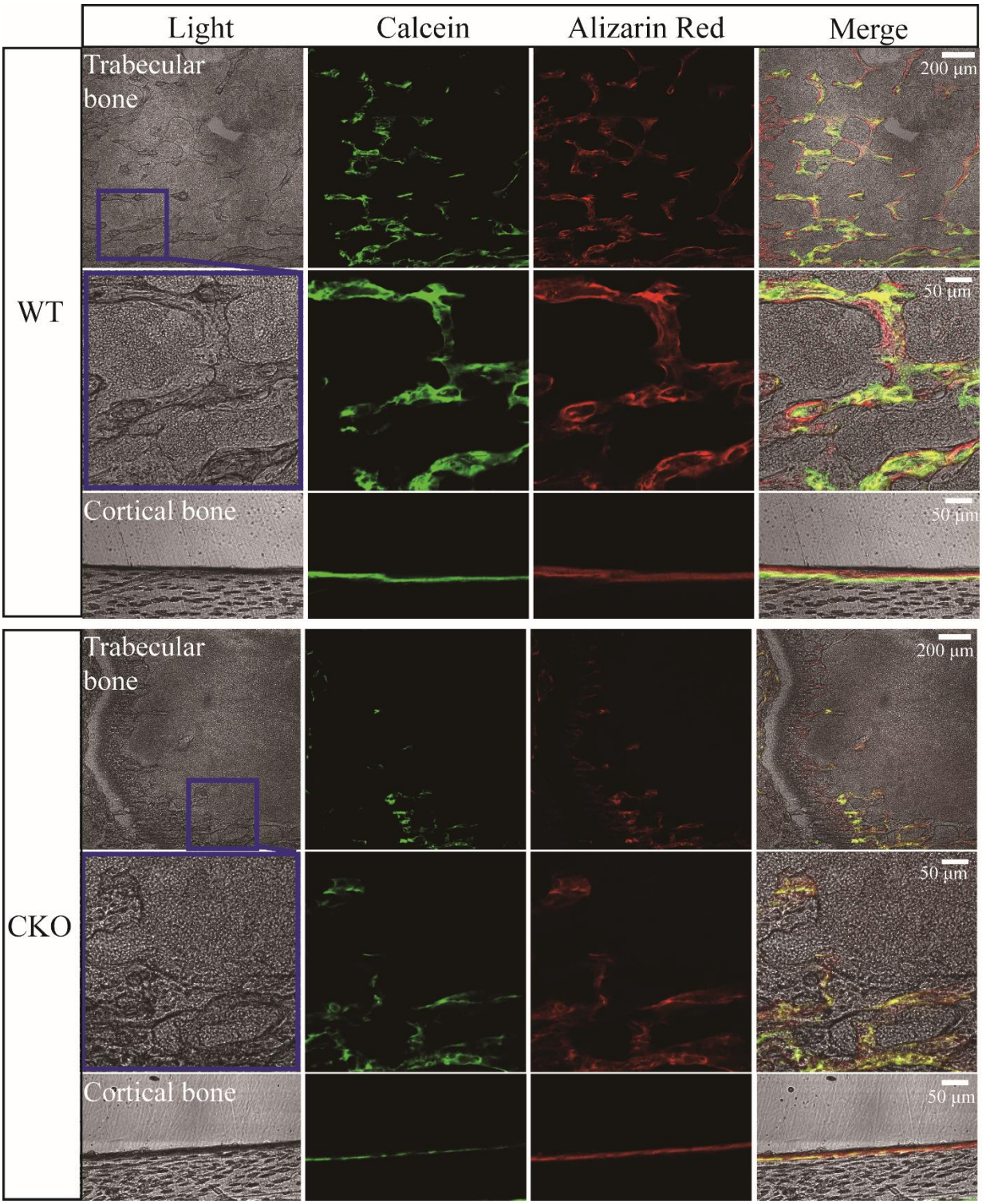

Appendix Figure 6. Double fluorescent labeling images of the trabecular and cortical bone surface of the femur in WT and CKO mice at 8 wk of age, supplemented for figure 3B in manuscript.

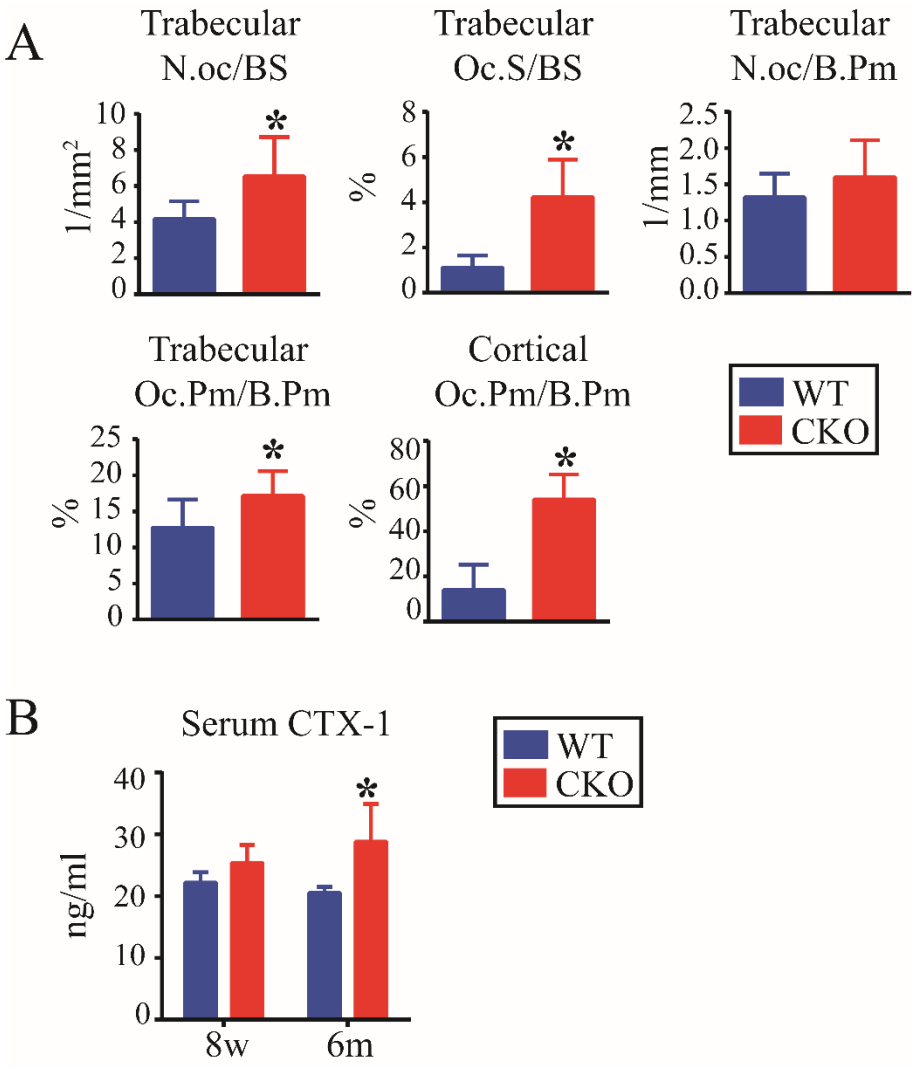

Appendix Figure 7. (A) Quantitative analysis of the number, size, perimeter of osteoclasts in the femur of WT and CKO mice at 8 wk of age. *P < 0.05, Student's t test, n=3. **(B)** CTX-I levels in WT and CKO mice at 8 wk and 6 mo of age. *P < 0.05, Student's t test, n=4.

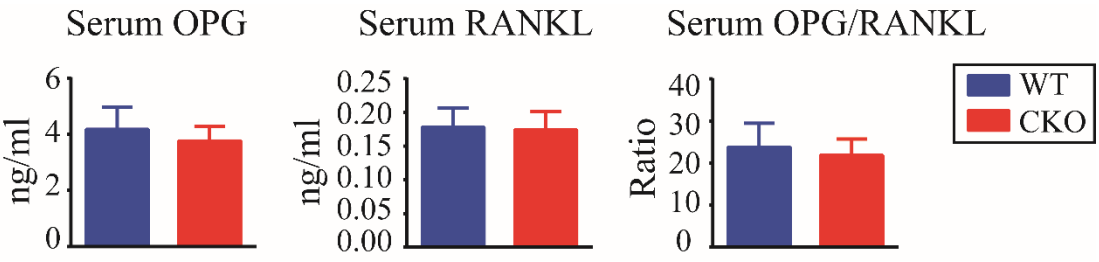

Appendix Figure 8. Serum RANKL and OPG level in WT and CKO mice at 8 wk of age. Student's t test, n=4.

Appendix References

Jarvinen TL, Sievanen H, Jokihaara J, Einhorn TA. 2005. Revival of bone strength: The bottom line. Journal of bone and mineral research : the official journal of the American Society for Bone and Mineral Research. 20(5):717-720.

Lu Y, Xie Y, Zhang S, Dusevich V, Bonewald LF, Feng JQ. 2007. Dmp1-targeted cre expression in odontoblasts and osteocytes. J Dent Res. 86(4):320-325.

Maycas M, Portoles MT, Matesanz MC, Buendia I, Linares J, Feito MJ, Arcos D, Vallet-Regi M, Plotkin LI, Esbrit P et al. 2017. High glucose alters the secretome of mechanically stimulated osteocyte-like cells affecting osteoclast precursor recruitment and differentiation. Journal of Cellular Physiology. 232(12):3611-3621.

Wang X, Wang S, Li C, Gao T, Liu Y, Rangiani A, Sun Y, Hao J, George A, Lu Y et al. 2012. Inactivation of a novel fgf23 regulator, fam20c, leads to hypophosphatemic rickets in mice. PLoS Genet. 8(5):e1002708.

Zhao S, Zhang YK, Harris S, Ahuja SS, Bonewald LF. 2002. Mlo-y4 osteocyte-like cells support osteoclast formation and activation. Journal of bone and mineral research : the official journal of the American Society for Bone and Mineral Research. 17(11):2068-2079.

Zhu X, Zhu H, Zhang L, Huang S, Cao J, Ma G, Feng G, He L, Yang Y, Guo X. 2012. Wls-mediated wnts differentially regulate distal limb patterning and tissue morphogenesis. Developmental Biology. 365(2):328-338.